

# Turbulent transport in the Madison Symmetric Torus reversed-field pinch\*

T. D. Rempel,<sup>†</sup> A. F. Almagri, S. Assadi, D. J. Den Hartog, S. A. Hokin, S. C. Prager, J. S. Sarff, W. Shen, K. L. Sidikman, C. W. Spragins, J. C. Sprott, M. R. Stoneking, and E. J. Zita

University of Wisconsin, Madison, Wisconsin 53706

(Received 22 November 1991; accepted 20 February 1992)

Measurements of edge turbulence and the associated transport are ongoing in the Madison Symmetric Torus (MST) reversed-field pinch [Fusion Technol. **19**, 131 (1991)] using magnetic and electrostatic probes. Magnetic fluctuations are dominated by  $m=1$  and  $n \sim 2R/a$ , tearing modes. Particle losses induced by magnetic field fluctuations have been found to be ambipolar ( $\langle \tilde{J}_{\parallel} \tilde{B}_r \rangle / B_0 = 0$ ). Electrostatic fluctuations are broadband and turbulent, with mode widths  $\Delta m \sim 3-7$  and  $\Delta n \sim 70-150$ . Particle, parallel current, and energy transport arising from coherent motion with the fluctuating  $\tilde{\mathbf{E}} \times \mathbf{B}$  drift have been measured. Particle transport via this channel is comparable to the total particle loss from MST. Energy transport (from  $\langle P \tilde{E}_{\phi} \rangle / B_0$ ) due to electrostatic fluctuations is relatively small, and parallel current transport (from  $\langle J_{\parallel} \tilde{E}_{\phi} \rangle / B_0$ ) may be small as well.

## I. INTRODUCTION

It has long been observed that plasma fluctuations in toroidal plasma confinement devices are large enough that correlated behavior could account for the observed anomalous transport. Indeed, measurements in tokamaks suggest that electrostatic fluctuations may induce a significant fraction of the particle and energy losses.<sup>1</sup> In addition, magnetic field fluctuations in a stochastic field coupled to parallel flows can be significant in some experiments. More insight into the origins of these fluctuations and the resulting transport can be had by comparison to the reversed-field pinch (RFP) plasma. Recent results have demonstrated that electrostatic particle transport may be important in the RFP as well.<sup>2-4</sup> The RFP exhibits similar equilibrium parameters to the tokamak, such as density, temperature, and edge gradients. However, the equilibrium magnetic topology of the RFP is distinct, with larger magnetic shear, unfavorable curvature, and a lower trapped particle fraction.

Identification of turbulent interactions which induce transport is facilitated by classification of the measurements by the correlation term. Electrostatic fluctuation-induced losses arise from fluctuations correlated with a radial  $\tilde{\mathbf{E}} \times \mathbf{B}$  particle drift. Similarly, fluctuations correlated with a stochastic fluctuating magnetic field,  $\tilde{B}_r$ , may also contribute to radial transport. The relevant correlation terms, listed in Table I,<sup>5</sup> quantify the losses regardless of the origins of these fluctuations. We have measured all or parts of the particle, current, and energy transport terms (1)-(4), and ascertain their role in determining confinement in the edge of the Madison Symmetric Torus (MST) RFP.

MST<sup>6</sup> is a large RFP, with  $R=1.5$  m,  $a=0.52$  m,  $I_p=600$  kA,  $\bar{n}=0.5-3 \times 10^{13}$  cm<sup>-3</sup>, and a pulse length of 60-80 msec. Plasma beta has been estimated to be

$\beta_p \leq 17\%$ , and the inferred particle and energy confinement times,  $\tau_p \lesssim \tau_E \sim 1$  msec. Measurements cited in this paper were made in low current plasmas ( $I_p=200-300$  kA) to allow probe insertion past the edge limiter ( $r/a=0.98$ ). Edge field errors, finite gyro-orbit effects, and other effects extend the edge scrape-off region to nearly  $r/a=0.92$ . For these plasmas, with reversal and pinch parameters,  $F \equiv B_{\phi}(a) / \langle B_{\phi} \rangle = -0.1$  to  $-0.2$  and  $\Theta \equiv B_{\theta}(a) / \langle B_{\phi} \rangle = 1.8$ , the central electron temperature has been measured to be  $T_{e0}=150-200$  eV, with radiated power fraction  $\sim 30\%$ . Analysis has also been restricted to time periods near peak current that do not exhibit sawtooth oscillations.<sup>7</sup>

The remainder of this paper is divided into five sections: Sec. II reviews edge measurements of magnetic and electrostatic fluctuations made in MST, Sec. III presents particle and energy loss measurements from fluctuations, Sec. IV discusses current transport and dynamo, Sec. V presents measurements of nonlinear wave interactions, and Sec. VI is a summary.

## II. OVERVIEW OF EDGE FLUCTUATIONS

Edge magnetic fluctuations in MST have been measured with fixed magnetic coil arrays at the wall and with insertable probes.<sup>8</sup> Two-point measurements of mode spectra are compatible with results from full arrays at the wall. In contrast to tokamaks, relative magnetic fluctuations are large,  $\tilde{B}/B_0 \sim 1-2\%$ . The dominant fluctuations occur at frequencies  $f < 30$  kHz, and have been identified as a poloidal  $m=1$ , and toroidal  $n \sim 2R/a$  global modes. The measured phasing of these modes is consistent with the tearing mode predictions by nonlinear magnetohydrodynamic (MHD) simulations, with toroidal and poloidal magnetic field fluctuations  $\pi$  out of phase, and  $\pi/2$  out of phase with radial magnetic field fluctuations.<sup>5</sup>

The high-frequency ( $f > 30$  kHz) fluctuations represent only a small fraction of the total power in the fluctuations, and correspond to modes locally resonant in the edge. The high-frequency (50-100 kHz)  $n$  spectra, deter-

\*Paper 515, Bull. Am. Phys. Soc. **36**, 2376 (1991).

<sup>†</sup>Invited speaker.

TABLE I. Correlation fluctuation quantities which can yield net radial transport (from Ref. 5). Negligible electron drift is assumed.

	Electrostatic	Magnetic
Particle	(1) $\frac{\langle \tilde{n}_{i,e} \tilde{E}_\perp \rangle}{B_0}$	(4) $\frac{\langle \tilde{j}_{i,e\parallel} \tilde{B}_r \rangle}{eB_0}$
Current	(2) $\frac{\langle \tilde{j}_\parallel \tilde{E}_\perp \rangle}{B_0}$	(5) $\frac{\langle \tilde{p}_\parallel \tilde{B}_r \rangle}{B_0}$
Energy	(3) $\frac{\langle \tilde{p}_e \tilde{E}_\perp \rangle}{B_0}$	(6) $\frac{\langle \tilde{Q}_\parallel \tilde{B}_r \rangle}{B_0}$

mined from a two-point toroidal measurement, at each of two radial locations ( $r=42$  and  $46$  cm) which bracket the toroidal magnetic field reversal surface ( $r\sim 44$  cm), are illustrated in Fig. 1(a) (it should be noted that two-point spectra will not detect correlated, simultaneous counter-propagating modes at the same frequency). The corresponding  $n$  spectra measured for all frequencies up to the Nyquist frequency are shown in Fig. 1(b). Measured high-frequency  $m$  spectra (not shown) do not show a similar change in sign. The measured ratio of mode numbers,  $m/n$ , changes sign with the field line pitch,  $q$ , as the probe is inserted deeper into the plasma and the toroidal magnetic field undergoes reversal. It is interesting to note that the

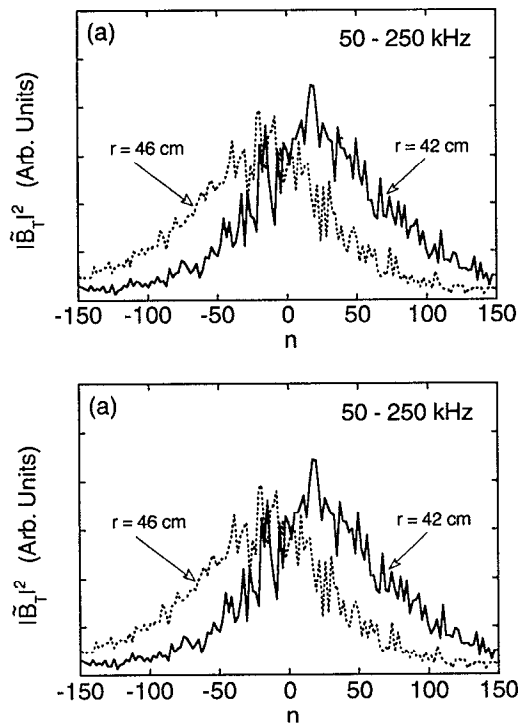


FIG. 1. Toroidal  $n$  mode spectra for  $\tilde{B}_r$ , measured at two radial positions ( $r=46$  cm, dashed line;  $r=42$  cm, solid line) which bracket the toroidal magnetic field reversal surface ( $r\approx 44$  cm) for (a) high-frequency (50–250 kHz) and (b) total (0–250 kHz) bandwidths.

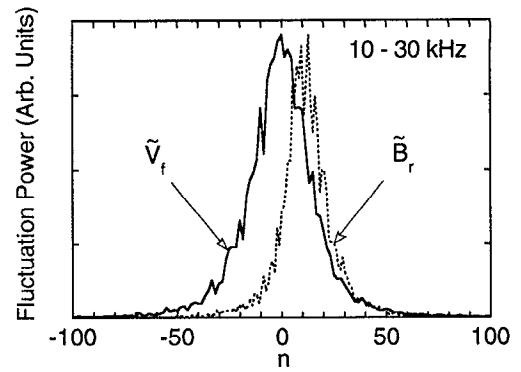


FIG. 2. Toroidal  $n$ -mode spectra for  $\tilde{V}_f$  and  $\tilde{B}_r$ , for  $f=10$ – $30$  kHz.

fluctuations maintain resonance by adjusting the sign of  $n$  (as opposed to  $m$ ), despite the fact that the propagation direction then reverses direction relative to the diamagnetic drift direction. Radial coherence lengths for these high-frequency modes have been measured to be small,  $\sim 1$  to  $3$  cm.

Total current density fluctuations have also been measured in the edge plasma in MST,<sup>9</sup> using a multicoil “forked” probe, through  $\mathbf{j}=\nabla\times\mathbf{B}$ . Typical uncertainties of  $<1\%$  in the magnetic measurements, arising from limitations in coil alignment and calibration, translate to uncertainties in the resulting fluctuating current of  $<15\%$  by this method. The current density fluctuation power peaks at low frequencies, with relative amplitudes for frequencies  $f<250$  kHz of  $\tilde{j}_\theta/j_{\theta 0}\sim 8\%$  and  $\tilde{j}_\parallel/j_{\parallel 0}\sim 4\%$ . Parallel current density fluctuations  $\tilde{j}_\parallel\sim\tilde{j}_\theta$ , and magnetic field fluctuations  $\tilde{B}_\parallel\sim\tilde{B}_\theta$ , are measured to be in phase, and the ratio of normalized fluctuations  $(\tilde{j}/j_0)/(\tilde{B}/B_0)\sim 4$ . These results are consistent with the relationship computed for the tearing mode oscillations. However, the computation predicts a higher level of fluctuations in a more narrow spectrum of  $n$  modes. This discrepancy may arise from the Lundquist number assumed in the code, which is nearly two orders of magnitude smaller than found in the experiment.

Edge electrostatic fluctuations in MST have been measured<sup>4</sup> with insertable Langmuir probes, using a triple probe technique. In general, the fluctuations are broadband and peaked at low frequencies. We find that fluctuation amplitudes are large and generally increase with radius, with relative plasma density fluctuations,  $\tilde{n}/n_0\sim 15\%$ – $35\%$ , and electron temperature fluctuations,  $\tilde{T}_e/T_{e0}\sim 10\%$ – $25\%$ . These levels are comparable to those found in tokamaks. Plasma potential fluctuations,  $\tilde{\Phi}_p$ , have been determined from vector addition of floating potential and electron temperature fluctuations, resulting in  $\tilde{\Phi}_p/T_{e0}\sim 20\%$ – $60\%$ . Pressure fluctuations have also been determined, allowing for phasing of density and temperature fluctuations. Within error bars, the Boltzmann relation,  $\tilde{p}_e/p_{e0}=e\tilde{\Phi}_p/T_{e0}$ , is not violated.

Mode spectra of the plasma potential are estimated from a two-point measurement of floating potential,  $\tilde{V}_f$ . The resulting spectra for  $f=10$ – $30$  kHz are broad,  $\Delta n\sim 70$ – $150$ , as shown in Fig. 2. Poloidal mode widths are

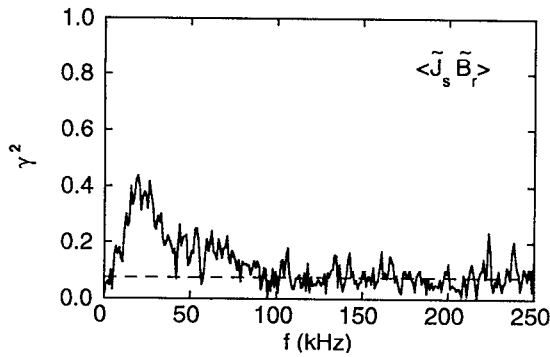


FIG. 3. Cross coherence,  $\gamma^2$ , measured between  $\tilde{J}_s$  and  $\tilde{B}_r$ , separated radially by 0.5 cm (solid line). The statistical level of significance is also plotted (dashed line).

$\Delta m \sim 3-7$ . The modes propagate toroidally in the ion drift direction with a phase velocity of  $v_{ph} \sim 5 \times 10^6$  cm sec $^{-1}$ . Measured spectra for ion saturation current,  $\tilde{J}_s$ , have been found to be generally similar to the  $\tilde{V}_f$  spectra. Although a complete Langmuir probe array is not available to determine the accuracy of the two-point method, measurements with probes separated from 0.28 cm to 4.3 cm give consistent results.

To the extent that magnetic field lines are frozen into the plasma, a fluctuating radial density convection accompanies radial magnetic field fluctuations. A fixed probe immersed in an equilibrium density gradient will then measure density fluctuations. Simultaneous measurements of magnetic and electrostatic fluctuations indicate only a modest correlation. The coherence ( $\gamma^2$ ) between  $\tilde{B}_r$  and  $\tilde{J}_s$ , shown in Fig. 3, peaks near the frequencies of the tearing mode at values of  $\gamma^2 \sim 0.4$  (true for  $\gamma^2$  between  $\tilde{V}_f$  and  $\tilde{B}_r$ , as well). Thus, a significant fraction of the measured density fluctuations may arise from sources other than radial convection with the magnetic field.

### III. PARTICLE AND ENERGY TRANSPORT

Particle transport of species  $i$  from correlated density turbulence and radial velocity fluctuations,  $\Gamma_i^{\text{fl}}$ , is given by

$$\Gamma_i^{\text{fl}} = \frac{\langle \tilde{n}_i \tilde{E}_\perp \rangle}{B_0} + \frac{\langle \tilde{j}_{i\parallel} \tilde{B}_r \rangle}{eB_0} = \Gamma_i^{\text{ES}} + \Gamma_i^{\text{M}},$$

where  $\tilde{E}_\perp$  is the electrostatic fluctuating field perpendicular to  $\mathbf{B}$ ,  $\tilde{j}_{i\parallel}$  is the fluctuating particle current parallel to  $\mathbf{B}$ , and  $B_0$  is the equilibrium value of  $\mathbf{B}$ . We have inferred the electrostatic fluctuation-induced electron flux  $\Gamma_i^{\text{ES}}$  from two-point correlations of Langmuir probe signals,  $\tilde{J}_s$ ,  $\tilde{V}_f$ , and  $T_e$ .<sup>4</sup> It is assumed the plasma potential can be represented by a superposition of waves with a unique dispersion  $k = k(\omega)$ , and that the perpendicular electrostatic electric field can be expressed as  $\tilde{E}_\perp = -ik_\perp(\tilde{V}_f + \alpha\tilde{T}_e)$ , where the wave vector  $k_\perp$  is determined from phasing between  $\tilde{V}_f$  signals and  $\alpha T_e$  is the sheath potential drop. As  $k_\perp$  is strongly polarized in the toroidal direction, the con-

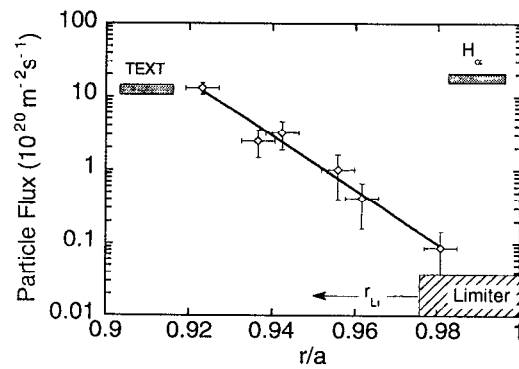


FIG. 4. Radial profile of edge electrostatic fluctuation-induced particle flux,  $\Gamma_i^{\text{ES}}$  (solid line) in MST. Peak edge electrostatic particle flux measured on TEXT (Ref. 10), and total edge losses in MST inferred from  $H_\alpha$  measurements are shown for comparison. The ion Larmor radius in MST is also illustrated.

tribution to particle flux from the measured poloidal electric fields is two orders of magnitude smaller and is ignored.

Contributions to the resulting flux are generally significant for frequencies below 50 kHz, with temperature fluctuations generating a modest component of the total flux. The radial dependence of  $\Gamma_i^{\text{ES}}$  for  $r/a = 0.92$  to  $0.98$  is shown in Fig. 4. The radial decay of this flux is consistent with a picture of increased parallel losses in a scrape-off layer with a scrape-off length to the edge toroidal limiter in MST. Also shown is the total particle loss rate determined from a one-dimensional (1-D) transport code using  $H_\alpha$  profile measurements, from which a particle confinement time of  $\tau_p \sim 1$  msec is inferred. We determine that electrostatic transport in the edge region (outside reversal) is significant when compared to particle losses from MST. Measurements of electrostatic transport in a similar sized tokamak<sup>10,11</sup> yield comparable losses, as illustrated in Fig. 4.

Particle losses in the edge due to correlated current and radial magnetic field fluctuations, as measured by the insertable "forked" magnetic pickup probe up to  $r/a = 0.82$ , have been determined to be ambipolar.<sup>9</sup> The magnitude of these fluctuations are large enough to cause significant transport,  $|\tilde{j}_\theta| |\tilde{B}_r| / eB_0 \sim 10^{21}$  m $^{-2}$  sec $^{-1}$ . However, the fluctuations  $j_\theta$  and  $\tilde{B}_r$  are measured to be nearly  $\pi/2$  out of phase at all frequencies (5–250 kHz), as shown in Fig. 5, yielding a net charge loss bounded by  $j/e \sim 5 \times 10^{19}$  m $^{-2}$  sec $^{-1}$ . Uncertainties in the phase measurement limit the error in this measured flux to an additional 5% of the total particle flux. The measured phase relation is expected for the tearing modes. Ambipolar transport is expected for localized modes which exhibit  $\tilde{B}_\perp B_0$ ,<sup>12</sup> so there is also reason to expect this relation to hold for the high-frequency modes as well.

The rate of particle loss of each species due to radial fluctuations in the magnetic field has not yet been determined. However, initial results utilizing a pinhole electron energy analyzer (EEA) indicate that the fluctuating fast electron current in MST might not contribute to particle

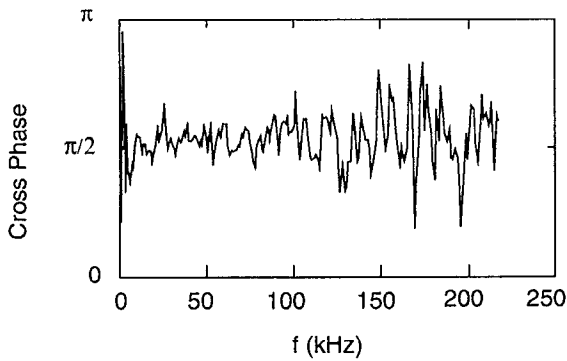


FIG. 5. Measured cross phase between total poloidal current  $\tilde{j}_\theta$  and  $\tilde{B}_r$  in the edge.

transport. When biased to collect electrons with energies  $>50$  eV, the EEA yields an electron current with fluctuations,  $j_{EEA}$ , which may also be  $\sim \pi/2$  out of phase with  $B_r$ . If these faster electrons dominate the total electron current, one would expect the flutter transport of ions to be small as well.

Electrostatic energy transport,  $Q_e^{ES}$ , is defined here as the heat flux due to correlated fluctuations in electron pressure  $p_e$  and radial  $\tilde{E} \times \mathbf{B}_0$  velocity. This has been measured in MST, and is relatively small.<sup>4</sup> The radial profile of  $Q_e^{ES}$  is shown in Fig. 6. Again, we interpret the radial falloff of this flux to arise from increased parallel losses. Of the  $\sim 100$  kW m<sup>-2</sup> (plasma surface area) of Ohmic input power,  $<30\%$  is lost through radiation at these low currents. The electrostatic fluctuation-induced heat flux represents only a small fraction,  $\leq 10\%$ , of the remainder. However, this measured flux is comparable to the  $\sim 10$  kW m<sup>-2</sup> attributed to electrostatic losses in a tokamak of similar size, where these losses dominate heat loss through plasma channels.<sup>13</sup>

Direct measurement of energy loss through magnetic fluctuations is difficult and has not been made. However, radial magnetic fluctuation amplitudes are large enough in RFP's so that this loss channel may be significant. The

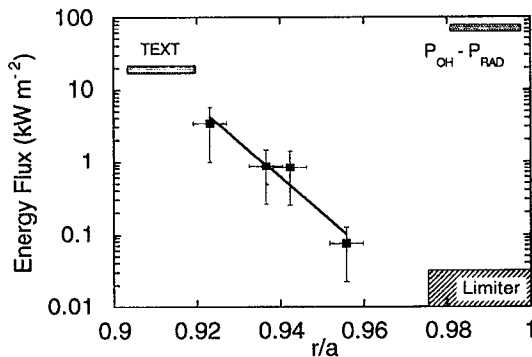


FIG. 6. Radial profile of edge electrostatic fluctuation-induced energy loss flux,  $Q_e^{ES}$  (solid line) in MST. Peak edge electrostatic energy flux for TEXT (Ref. 12) and total nonradiative losses for MST are shown for comparison.

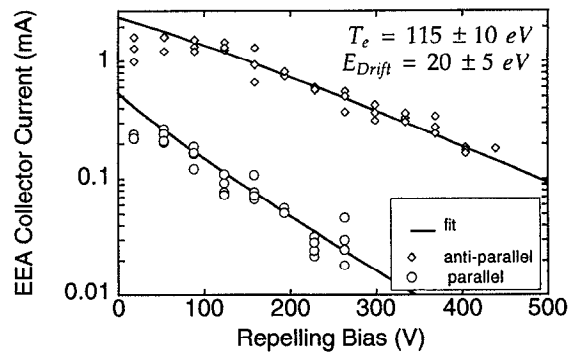


FIG. 7. Pinhole energy analyzer signal for current directed parallel ( $\diamond$ ), and antiparallel ( $\circ$ ) to peak hot electron current, and single drifted Maxwellian distribution fit (—) with three fit parameters: a temperature of  $T_e = 115$  eV, a drift energy of  $\frac{1}{2}mv_d^2 = 20$  eV, and an effective density of  $10^{11}$  cm<sup>-3</sup>.

energy confinement time estimated from turbulence in stochastic magnetic fields<sup>14</sup> is comparable to global energy confinement times in MST.

#### IV. CURRENT TRANSPORT

Radial transport of field-aligned current which balances in large part the resistive diffusion, and thereby sustains toroidal field reversal, is of particular interest for the RFP. The process also has relevance to tokamaks, where the dynamics which control current diffusion and profile shaping are important. The RFP dynamo has long been considered to arise from coherent MHD fluid velocity fluctuations generating an effective parallel electric field (“MHD dynamo”),  $E_{\parallel} \sim (\tilde{\mathbf{u}} \times \tilde{\mathbf{B}})_{\parallel}$ . This view is supported by a large body of theoretical work.<sup>15-18</sup> A kinetic “dynamo” has more recently been proposed,<sup>19</sup> in which the current is carried by free-streaming electrons accelerated along the stochastic magnet field. This model was suggested by the observation of hot electrons streaming along field lines in the edge plasma of ZT40,<sup>20</sup> with temperatures in excess of the central electron temperature. The total edge currents have been attributed to these particles.

Hot electrons have also been observed in the edge plasma of MST with a pinhole electron energy analyzer. Langmuir probe measurements indicate a local electron temperature of 20 to 30 eV. The measured energy dependence of field-aligned hot electrons can be approximated by a drifted Maxwellian distribution with a temperature of  $T_{e\parallel} \sim 115$  eV  $< T_{e0}$  and a drift energy of  $\frac{1}{2}mv_{\parallel}^2 \sim 20$  eV as shown in Fig. 7. The collecting efficiency of the analyzer is nonlinear at low repelling bias, resulting in a poor fit at these bias levels. It has not yet been determined whether or not the edge current is predominantly carried by these hot electrons, although the possibility remains within the uncertainties of the diagnostic.

“Electrostatic” current transport due to coherent oscillations between the fluctuating parallel current and perpendicular electric-field-induced drift is proportional to  $\Gamma_j^{ES} \sim \langle \tilde{E}_\phi \tilde{j}_\theta \rangle / B_0$ . Although there is no theoretical basis on which to expect this term to be significant, the relative size

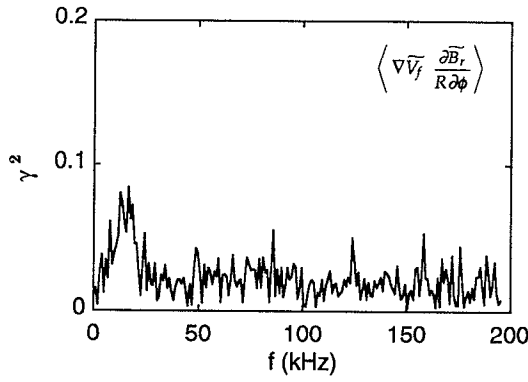


FIG. 8. Coherence between the fluctuating electric field component,  $-\nabla \tilde{V}_f$  and the fluctuation poloidal current component,  $\partial \tilde{B}_r / R \partial \phi$ .

of the fluctuations makes it difficult to discount outright. We have measured  $\tilde{j}_\theta / j_0 \sim 0.08$ , and  $\tilde{E}_\phi / E_0 \sim 50$ , where  $E_0 = V_f / 2\pi R$ . If the correlation is high, a term nearly four times the Ohmic dissipation would result.

Initial measurements of electrostatic current transport,  $\langle \tilde{E}_r \tilde{j}_\parallel \rangle \sim \langle \tilde{E}_\phi \tilde{j}_\theta \rangle$  indicate that this term may be small. Measurements were made with Langmuir and magnetic probes separated by 6 cm in the poloidal direction (well within poloidal correlation lengths) and  $\leq 1$  cm in the radial direction. Radial correlation lengths for magnetic fluctuations are significantly larger than this separation, except at higher frequencies,  $f > 100$  kHz, where they become comparable. With these assumptions,  $\Gamma_j^{\text{ES}}$  can be expressed as

$$\Gamma_j^{\text{ES}} \cong \frac{4\pi}{cB_0} \left\langle -ikV_f \left( \tilde{V}_f + \alpha \frac{k_B}{e} \tilde{T}_e \right) \times \left( \frac{\partial \tilde{B}_r}{\partial r} - ik_B \tilde{B}_r \right)^* \right\rangle,$$

where  $k_B$  is the wave number of  $\tilde{B}_r$ . Computation of this flux is then composed of four terms, of which  $\langle k_V \tilde{V}_f k_{BR} \tilde{B}_r^* \rangle$  appears to dominate.

The coherence between the electric field component,  $-ik_V \tilde{V}_f$ , and the poloidal current component,  $ik_B \tilde{B}_r / \omega$  plotted in Fig. 8, however, is small. This is defined

$$\gamma_{jE}^2 = \frac{\langle k_V \tilde{V}_f k_{BR} \tilde{B}_r^* \rangle}{|k_V \tilde{V}_f| |k_{BR} \tilde{B}_r|}.$$

This coherence peaks at  $\leq 8\%$ , yielding a term which is  $\leq 15\%$  of the Ohmic dissipation. The terms proportional to the radial gradient in  $\tilde{B}_\phi$  are presently measured with large error bars, and as of yet cannot be reported with confidence. These initial results, however, indicate that the electrostatic fluctuation-induced transport of parallel current may be small.

## V. NONLINEAR COUPLING

Nonlinear wave coupling of magnetic fluctuations has been directly measured in MST,<sup>7</sup> and results are in good agreement with numerical simulations. Experimental mea-

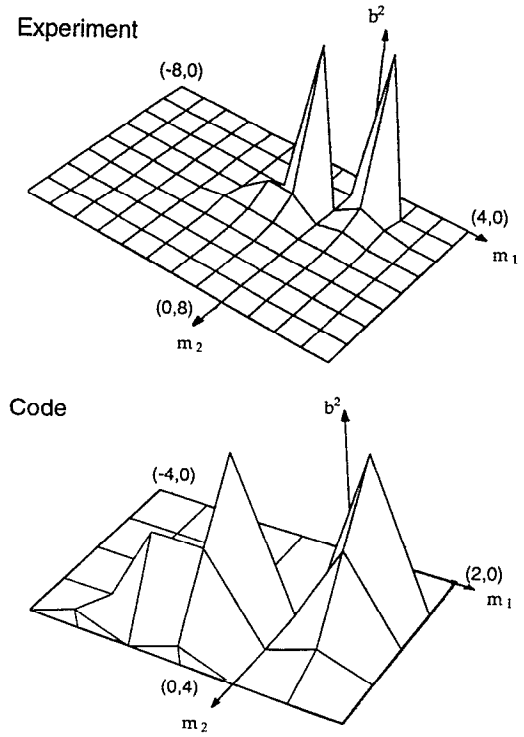


FIG. 9. Poloidal three-wave coupling of  $\tilde{B}_\theta$ , as measured by bicoherence,  $b^2(m_1, m_2, m_1 + m_2)$ .

surements have utilized a poloidal and toroidal array of wall-mounted magnetic pickup coils, which are limited to mode numbers  $m < 8$  and  $n < 32$ . Three-wave coupling is determined by calculating the bicoherence,  $b^2$ , which is defined

$$b^2 = \frac{\langle X(m_1 + m_2) X^*(m_1) X^*(m_2) \rangle}{|X(m_1) X(m_2)| |X(m_1 + m_2)|},$$

where  $X$  is the spatial Fourier transform of the measured signal. The same statistical analysis is performed on the output of a cylindrical, three-dimensional (3-D), nonlinear resistive MHD code, which is run many times with varying initial conditions. As illustrated in Fig. 9, measurements of poloidal wave coupling in the poloidal component of the fluctuating magnetic field yield nearly identical results, with the dominant coupling occurring between  $m = |1|$  and 2 modes. However, the computation does not include mode coupling from toroidal effects, which can contribute to the presence of  $m = 2$  modes. The bicoherence for the toroidal modes is shown in Fig. 10, where strong coupling is observed for modes  $n < 20$ . In both cases, the coupling is strongest between the  $n = 5-8$  modes. Phase locking of these modes is typically observed in MST. The code predicts coupling between fewer modes than is measured in the experiment, which again may be due to disparate Lundquist numbers. During the time period immediately preceding the sawtooth oscillations in MST, a dramatic increase in the nonlinear coupling of higher and lower  $n$  is directly measured, and the  $n$ -mode spectrum is distinctly

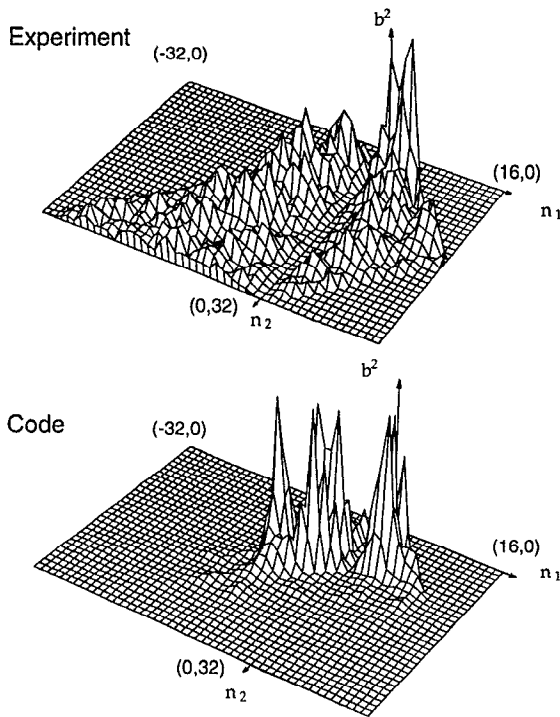


FIG. 10. Toroidal three-wave coupling of  $\tilde{B}_0$ , as measured by bicoherence,  $b^2(n_1, n_2, n_1 + n_2)$ .

broadened. In addition to this change in toroidal activity, an increase in poloidal coupling of higher  $m$  modes is measured.

## VI. SUMMARY

Studies of fluctuation-induced transport are ongoing in MST. We have measured the contributions of electrostatic  $\tilde{E} \times B_0$  drifts to particle, energy, and current transport in the edge region, and have made advances in the understanding of magnetic fluctuation-induced losses. Electrostatic fluctuation-induced edge particle transport is comparable to total edge particle losses for the RFP, as in the tokamak. Edge energy and current transport via similar channels appear to be relatively small in the RFP, but are comparable in magnitude to similar measurements in the tokamak. Energy loss through magnetic fluctuations is expected to dominate in the RFP (and be negligible in the tokamak edge), but this quantity is difficult to measure

directly. Magnetic flutter transport of particles is directly measured to be ambipolar in the RFP, and losses through higher energy electron currents may also be small. Nonlinear mode coupling has been directly measured in MST, and is comparable with numerical simulations.

## ACKNOWLEDGMENTS

The authors are extremely grateful to James Callen, Paul Terry, and Nathan Mattor for useful discussions.

Saeed Assadi acknowledges the support of the AT&T Corporation and the National Science Foundation for Nonlinear Studies. This work is supported by the U.S. Department of Energy.

<sup>1</sup>See, for example, A. J. Wooton, B. A. Carreras, H. Matsumoto, K. McGuire, W. A. Peebles, Ch. P. Ritz, P. W. Terry, and S. J. Zweben, *Phys. Fluids B* **2**, 2879 (1990).

<sup>2</sup>H. Ji, H. Toyama, K. Miyamoto, S. Shinohara, and A. Fujisawa, *Phys. Rev. Lett.* **67**, 62 (1991).

<sup>3</sup>H. Y. W. Tsui, Ch. P. Ritz, G. Miller, J. C. Ingraham, C. P. Munson, K. F. Schoenberg, and P. G. Weber, *Nucl. Fusion* **31**, 2371 (1991).

<sup>4</sup>T. D. Rempel, C. W. Spragins, S. C. Prager, S. Assadi, D. J. Den Hartog, and S. Hokin, *Phys. Rev. Lett.* **67**, 1438 (1991).

<sup>5</sup>S. C. Prager, *Plasma Phys. Controlled Fusion* **32**, 903 (1990).

<sup>6</sup>R. N. Dexter, D. Kerst, T. W. Lovell, S. C. Prager, and J. C. Sprott, *Fusion Technol.* **19**, 131 (1991).

<sup>7</sup>S. Hokin, A. Almagri, S. Assadi, J. Beckstead, G. Chartas, N. Crocker, M. Cudzinovic, D. Den Hartog, R. Dexter, D. Holly, S. Prager, T. Rempel, J. Sarff, E. Scime, W. Shen, C. Spragins, G. Starr, M. Stoneking, and C. Watts, *Phys. Fluids B* **3**, 2241 (1991).

<sup>8</sup>A. Almagri, S. Assadi, J. Beckstead, G. Chartas, N. Crocker, D. Den Hartog, R. Dexter, S. Hokin, D. Holly, E. Nilles, S. Prager, T. Rempel, J. Sarff, E. Scime, C. Spragins, J. Sprott, G. Starr, M. Stoneking, and C. Watts, in *Proceedings of the Workshop on Physics of Alternative Confinement Schemes*, Varenna, Italy, 1990, edited by S. Ortolani and E. Sidoni (Società Italiana di Fisica, Bologna, 1991), p. 223.

<sup>9</sup>W. Shen, R. N. Dexter, and S. C. Prager, *Phys. Rev. Lett.* **68**, 1319 (1992).

<sup>10</sup>K. W. Gentle, *Nucl. Technol./Fusion* **1**, 479 (1981).

<sup>11</sup>W. L. Rowan, C. C. Klepper, Ch. P. Ritz, R. D. Bengtson, K. W. Gentle, P. E. Phillips, T. L. Rhodes, B. Richards, and A. J. Wooton, *Nucl. Fusion* **27**, 1105 (1987).

<sup>12</sup>R. E. Waltz, *Phys. Fluids* **25**, 1269 (1982).

<sup>13</sup>Ch. P. Ritz, R. V. Bravenec, P. M. Schoch, R. D. Bengtson, J. A. Boedo, J. C. Forster, K. W. Gentle, Y. He, R. L. Hickok, Y. J. Kim, H. Lin, P. E. Phillips, T. L. Rhodes, W. L. Rowan, P. M. Valanju, and A. J. Wooton, *Phys. Rev. Lett.* **62**, 1844 (1989).

<sup>14</sup>A. B. Rechester and M. N. Rosenbluth, *Phys. Rev. Lett.* **40**, 38 (1978).

<sup>15</sup>A. Aydemir and D. C. Barnes, *Phys. Rev. Lett.* **52**, 930 (1984).

<sup>16</sup>H. R. Strauss, *Phys. Fluids* **27**, 2580 (1984).

<sup>17</sup>E. J. Caramana and D. D. Schnack, *Phys. Fluids* **26**, 1305 (1986).

<sup>18</sup>J. Dahlberg, D. Montgomery, G. D. Doolen, and L. Turner, *J. Plasma Phys.* **40**, 39 (1988).

<sup>19</sup>A. R. Jacobson and R. W. Moses, *Phys. Rev. A* **29**, 335 (1984).

<sup>20</sup>J. C. Ingraham, R. F. Ellis, J. N. Dowing, C. P. Munson, P. G. Weber, and G. A. Wurden, *Phys. Fluids B* **2**, 143 (1990).